J|A|C|S
ARTICLES

Published on Web 08/12/2008

Reversible Structural Transition in MIL-53 with Large Temperature Hysteresis

Yun Liu,*,†,‡ Jae-Hyuk Her,†,‡ Anne Dailly,§ Anibal J. Ramirez-Cuesta,|| Dan A. Neumann,† and Craig M. Brown*,†

NIST Center for Neutron Research, 100 Bureau Drive, Gaithersburg, Maryland, Department of Materials Science and Engineering, University of Maryland, College Park, Maryland, Chemical and Environmental Sciences Laboratory, General Motors Corporation, Warren, Michigan, and ISIS Facility, CCLRC Rutherford Appleton Laboratory, Chilton OX11 0QX, United Kingdom

Received May 16, 2008; E-mail: craig.brown@nist.gov; yunliu@nist.gov

Abstract: The metal-organic framework, MIL-53, can have a structural transition from an open-pored to a closed-pored structure by adsorbing different guest molecules. The aid of guest molecules is believed to be necessary to initiate this "breathing" effect. Using both neutron powder diffraction and inelastic neutron scattering techniques, we find that MIL-53 exhibits a reversible structural transition between an open-pored and a closed-pored structure as a function of temperature without the presence of any guest molecules. Surprisingly, this structural transition shows a significant temperature hysteresis: the transition from the open-pored to closed-pored structure occurs at approximately 125 to 150 K, while the transition from the closed-pored to open-pored structure occurs around 325 to 375 K. To our knowledge, this is first observation of such a large temperature hysteresis of a structural transition in metal-organic frameworks. We also note that the transition from the open to closed structure at low temperature shows very slow kinetics. An ab initio computer simulation is employed to investigate the possible mechanism of the transition.

I. Introduction

Due to the design and synthesis flexibility inherent in metal-organic frameworks (MOFs), there have been many efforts to address technological applications using these materials in categories such as gas adsorption,[1−8] gas selectivity,[9] and catalysis.[10] Especially, many MOFs can be tailored to have very large internal void-space with tunable pore sizes, which is very useful for gas storage,[1−7] including hydrogen storage.[1−6] Although the crystal structures of MOFs are typically composed of rigid frameworks, they can demonstrate significant structural distortions upon adsorption/desorption of guest molecules.[8,9,11,12] An extreme aspect of this type of distortion occurs as a "breathing" effect that is typically associated with a large change of the internal pore volume and has recently attracted significant research interest. For example, the MIL-88 class of flexible solids was shown to have different open-pored structures upon adsorbing different guest molecules. In this case, the cell volume of the larger analogue can more than triple from ∼2480 Å^3 to ∼8240 Å^3.[12] The volume change due to this breathing effect is significantly larger than that observed in earlier hybrid solids.[11,12]

MIL-53, which is made up of corner-sharing metal (Cr or Al) clusters interconnected with benzenedicarboxylate (BDC) organic ligands,[11,13] has also shown reversible structural changes due to the framework interaction with guest molecules. Upon removal of solvent molecules by evacuating the sample at moderate temperatures, MIL-53 has an open structure with a large internal volume.[11,13] However, at room temperature, it adsorbs water, significantly reducing the volume of the unit cell by shrinking the pores.[11,13] Recently, it has been shown that MIL-53 can also adsorb large amount of CO_2 and CH_4,[8] which have been characterized using in situ X-ray diffraction and infrared spectroscopy techniques.[14] Interestingly, the hydrated MIL-53 can selectively adsorb CO_2 over CH_4.[9] All of these features are intrinsically due to the reversible breathing of the

† NIST Center for Neutron Research.
‡ Department of Materials Science and Engineering, University of Maryland.
§ Chemical and Environmental Sciences Laboratory, General Motors Corporation.
|| ISIS Facility, CCLRC Rutherford Appleton Laboratory.

(1) Wong-Foy, A. G.; Matzger, A. J.; Yaghi, O. M. *J. Am. Chem. Soc.* **2006**, *128*, 3494.
(2) Latroche, M.; Surblé, S.; Serre, C.; Mellot-Draznieks, C.; Llewellyn, P. L.; Lee, J. H.; Chang, J. S.; Jhung, S. H.; Férey, G. *Angew. Chem., Int. Ed.* **2006**, *45*, 8227.
(3) Dincă, M.; Dailly, A.; Liu, Y.; Brown, C. M.; Neumann, D. A.; Long, J. R. *J. Am. Chem. Soc.* **2006**, *128*, 16876.
(4) Dincă, M.; Han, W. S.; Liu, Y.; Dailly, A.; Brown, C. M.; Long, J. R. *Angew. Chem., Int. Ed.* **2007**, *46*, 1419.
(5) Lin, X.; Jia, J.; Zhao, X.; Thomas, K. M.; Blake, A. J.; Walker, G. S.; Champness, N. R.; Hubberstey, P.; Schröder, M. *Angew. Chem.* **2006**, *118*, 1.
(6) Ma, S.; Sun, D.; Ambrogio, M.; Fillinger, J. A.; Parkin, S.; Zhou, H. C. *J. Am. Chem. Soc.* **2006**, *129*, 1858.
(7) Férey, G.; Latroche, M.; Serre, C.; Millange, F.; Loiseau, T.; Percheron-Guégan, A. *Chem. Comm.* **2003**, 2976.
(8) Bourrelly, S.; Llewellyn, P. L.; Serre, C.; Millange, F.; Loiseau, T.; Férey, G. *J. Am. Chem. Soc.* **2005**, *127*, 13519.
(9) Llewellyn, P. L.; Bourrelly, S.; Serre, C.; Filinchuk, Y.; Férey, G. *Angew. Chem., Int. Ed.* **2006**, *45*, 7751.
(10) Wu, C. D.; Hu, A.; Zhang, L.; Lin, W. *J. Am. Chem. Soc.* **2005**, *127*, 8940.
(11) Serre, C.; Millange, F.; Thouvenot, C.; Noguès, M.; Marsolier, G.; Louër, D.; Férey, G. *J. Am. Chem. Soc.* **2002**, *124*, 13519.
(12) Serre, C.; Mellot-Draznieks, C.; Surblé, S.; Audebrand, N.; Filinchuk, Y.; Férey, G. *Science* **2007**, *315*, 1828.
(13) Loiseau, T.; Serre, C.; Huguenard, C.; Fink, G.; Taulelle, F.; Henry, M.; Bataille, T.; Férey, G. *Chem. Eur. J.* **2004**, *10*, 1373.

MIL-53 framework. DFT computer simulations, together with X-ray diffraction experiments, indicate that host−guest interactions are responsible for these structural transformations at room temperature. Especially, the hydroxyl group of MIL-53 plays a major role during the structural transition.[14a,15]

In this paper, we show that MIL-53(Al) has a reversible structural transition from an open-pored to a closed-pored structure as a function of temperature and that the transitions are due to the intrinsic properties of MIL-53(Al) without the aid of any guest molecules. More interestingly, we have observed that the structural breathing shows an exceptionally large temperature hysteresis. We have identified the temperature hysteresis diagram of MIL-53(Al) structure using inelastic neutron scattering. An important consequence of this temperature hysteresis is that the biphasic composition of an MIL-53(Al) sample at room temperature depends on the sample's thermal history. This observation significantly affects many measurements that require an accurate measure of the internal volume of the material. In addition, the transition rate from the open structure to the closed structure at 77 K is very slow and on the time scale of typical volumetric adsorption experiments. We have used first principle calculations to better understand the driving force for the phase transition.

II. Materials and Methods

Synthesis and Chemical Characterization. MIL-53(Al) was synthesized according to the synthesis method and conditions (molar ratio, time and temperature) described in the literature.[7,13] The sample was prepared by hydrothermal reaction between the nitrate salt of the metal ion ($Al(NO_3)_3.9H_2O$) and terephthalic acid (1,4-benzenedicarboxylic acid, H_2BDC) in a Teflon-lined stainless steel Parr bomb. The as-synthesized powders were then rinsed with deionized water. Further activation treatments were performed on the as-synthesized materials in order to remove the unreacted acid present outside and within the pores.[13] Free terephthalic acid filling the pores of as-synthesized MIL-53(Al) was removed by calcination. We found that both free and occluded BDC molecules needed either a longer time or a much higher temperature than the published procedure of heating 300−320 °C in air for 3 days.[13]

MIL-53(Al) samples were characterized using powder X-ray diffraction and thermogravimetric analysis. X-ray diffraction patterns and TGA curves obtained on the synthesized and further activated samples were successfully compared to reported characterization data.

Sample masses ranged from 100 to 200 mg for gas-sorption measurements. The specific surface areas (SSA) of the samples evaluated from nitrogen sorption isotherms at 77 K were about 1270 $m^2 \cdot g^{-1}$ and 1580 $m^2 \cdot g^{-1}$, according to the BET (Brunauer−Emmett−Teller) and Langmuir models respectively. The measured values are in good agreement with published data.[13] Excess adsorption isotherms are based upon the equation-of-state of hydrogen[16] using a room temperature helium calibration of the system volume when the dehydrated sample was in the high temperature phase.

Neutron Powder Diffraction. Neutron powder diffraction experiments were performed at the National Institute of Standards and Technology Center for Neutron Research (NCNR) using the BT-1 diffractometer and neutrons of a wavelength of 2.0787 Å. The dehydrated sample was further degassed using a turbomolecular pump at a temperature of 120 °C overnight, and then 700 mg was transferred into a vanadium cell sealed with an indium O-ring in a helium glovebox. Any adsorbed He gas was pumped out using a turbomolecular vacuum pump when the sample cell was mounted to the sample stick. The sample was not exposed to air during sample handling and was maintained under vacuum during all neutron experiments. A top-loading closed-cycle refrigerator (CCR) was used to control the sample temperature. A temperature sensor mounted immediately above the sample cell recorded the sample temperature. Diffraction patterns were collected at four temperatures with each measurement taking about 8 h. The temperatures were (in order of measurement) 450, 295, 77, and 295 K.

Inelastic Neutron Scattering. Inelastic neutron scattering (INS) spectra were measured as a function of temperature using the time-of-flight Disk Chopper Spectrometer (DCS) and Fermi Chopper Spectrometer (FCS) at the NCNR. The same sample, cell, and top-loading CCR used in the neutron powder diffraction experiments were used in the INS experiments. For the DCS experiments, we measured the spectra of MIL-53(Al) at room temperature after thermally cycling the sample to 450 K and subsequently after quenching the sample in liquid nitrogen and heating back to room temperature. Measurements were taken with an incident wavelength of 6 Å resulting in a useful momentum transfer range (Q) of 0.4 $Å^{-1}$ to 2.85 $Å^{-1}$. Data were summed over the elastic line to obtain the diffraction pattern, and summed over Q to obtain the inelastic spectra. For the FCS experiments, the measurement temperatures followed the following sequence: 450, 370, 350, 320, 390, 420, 295, 250, 200, 150, 250, 295, 320, 350, and 390 K. Data were collected at a wavelength of 6 Å and summed over all Q for each temperature. Each measurement at FCS took more than 10 h. The filter-analyzer spectrometer (FANS) at the NCNR was used to measure the density of states of MIL-53(Al) with energy transfer from about 47 to 180 meV (see Supporting Information for details).

DFT Calculations. We performed Density Functional Theory (DFT) calculations using the LDA functional,[17] plane waves and periodic boundary conditions.[18] The structures were relaxed to the positions of minimum energy keeping the lattice parameters fixed at the experimental values. We used a plane wave energy cutoff of 460 eV, the reciprocal space was sampled with a Monkhorst-Pack scheme using a k-point mesh of spacing <0.05 $Å^{-1}$ for all phases and Vanderbilt ultrasoft pseudopotentials for the atoms and the finite displacement method for the calculation of the dynamical properties. We used the default convergence parameters for the ultrafine settings (see Supporting Information). INS spectra were produced using published methodologies.[19]

III. Results and Discussions

The degassed sample was investigated using neutron powder diffraction with the first diffraction pattern obtained at 450 K. Using the reported high-temperature orthorhombic structure[13] (space group: *Imma*), gives an excellent fit to the pattern with goodness-of-fit parameter of $\chi^2 = 1.03$, $R_{wp} = 4.545\%$, and $R_p = 3.433\%$ (see Supporting Information for details, Table S1 and Figure S1). This phase of MIL-53(Al) has the open-pored structure. The unit cell parameters are $a = 6.6361(5)$ Å, $b = 16.744(2)$ Å, $c = 12.847(2)$ Å with a unit cell volume of 1427.5(3) $Å^3$ and an accessible pore volume of ~393 $Å^3$ (see Supporting Information). A similar transition to an open-pored structure upon heating has also been observed for MIL-88.[12] Using the same terminology in previous publications,[13,14] we denote this high temperature phase as the HT phase. Figure 1(a) shows the powder diffraction pattern and Rietveld refinement

(14) (a) Serre, C.; Bourrelly, S.; Vimont, A.; Ramsahye, N. A.; Maurin, G.; Llewellyn, P. L.; Daturi, M.; Filinchuk, Y.; Leynaud, O.; Barnes, P.; Férey, G. *Adv. Mater.* **2007**, *19*, 2246. (b) Vimont, A.; Travert, A.; Bazin, P.; Lavalley, J. C.; Daturi, M.; Serre, C.; Férey, G.; Bourrelly, S.; Llewellyn, P. L. *Chem. Commun.* **2007**, 3291–3293.
(15) Ramsahye, N. A.; Maurin, G.; Bourrelly, S.; Llewellyn, P.; Loiseau, T.; Férey, G. *Phys. Chem. Chem. Phys.* **2007**, *9*, 1059.
(16) NIST Standard Reference Database 23: NIST Reference Fluid Thermodynamic and Transport Properties Database.
(17) Ceperley, D. M.; Alder, B. J. *Phys. Rev. Lett.* **1980**, *45*, 566.
(18) Clark, S. J.; Segall, M. D.; Pickard, C. J.; Hasnip, P. J.; Probert, M. J.; Refson, K.; Payne, M. C. *Z. Kristallogr.* **2005**, *220*, 567.
(19) Ramirez-Cuesta, A. J. *Comput. Phys. Commun.* **2004**, *157*, 226.

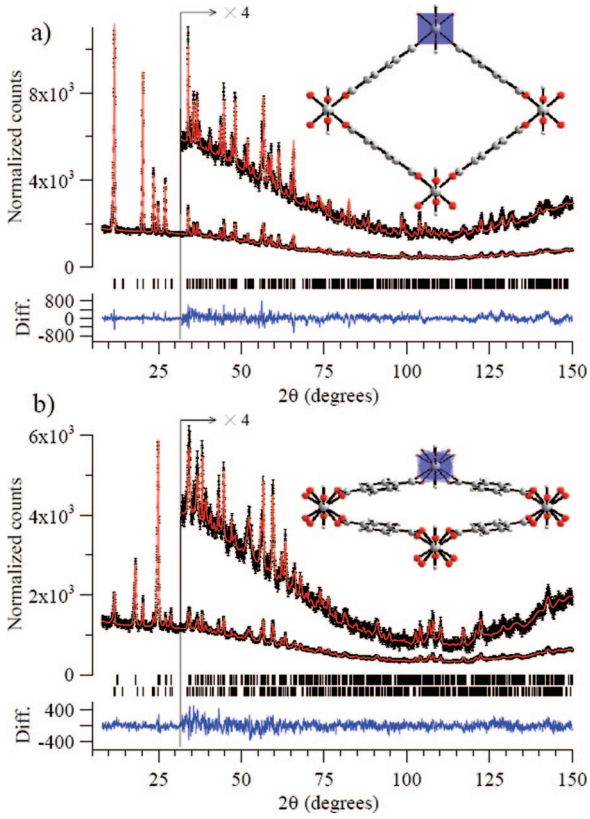

Figure 1. Neutron powder diffraction data (black points) of MIL-53(Al) collected at room temperature after heating to 450 K (upper) and cooling to 77 K (lower). MIL-53(Al) exists either as an open-pored (HT) phase or a predominantly closed-pored phase (LT), depending on the thermal history. The solid red lines are Rietveld refinement fits to the data using the structural models given in the text and illustrated in the inset. Vertical markers give Bragg peak positions for the respective phases and the solid line beneath is the difference between the experimental and calculated intensities. Note the scaling factor applied to the upper patterns and the difference data for angles greater than 26°. Error bars in the experimental data indicate one standard deviation of the counting statistics.

fits upon cooling the sample to 295 K. The lattice parameters at 295 K are very similar to those at 450 K indicating that the HT structure is stable upon cooling and throughout the measurement at room temperature.

Previous studies have identified adsorbed guest molecules as the key factor in triggering the transition of MIL-53(Al) from an open-pored, HT phase to a solvated closed-pored, or low temperature (LT) phase.[13,14] However, as evidenced from the diffraction patterns taken on cooling the sample to 77 K (see Supporting Information, Table S1 and Figure S2), MIL-53(Al) has mostly transformed from the HT phase to a closed-pore structure without adsorbing any guest molecules. The new majority phase present at 77 K (88% phase fraction) is monoclinic (space group *C2/c*, lattice parameters: $a = 20.824(1)$ Å, $b = 6.871(1)$ Å, $c = 6.6067(5)$ Å) and very similar to the room temperature framework structure of MIL-53(Al) with adsorbed water or CO_2.[9,11,13,14] While this phase is not solvated, we will extend the terminology already in the literature and refer to the closed-pored phase irrespective of solvation state as MIL-53(LT). With a value of 863.9(2) Å^3, the unit cell volume for the new LT phase has significantly decreased from that of the HT phase with almost zero available pore volume for adsorption of hydrogen (see Supporting Information). The appearance of the LT phase by 77 K is quite unexpected since all previous publications have indicated that a guest-framework interaction is necessary to foster the transformation to the narrow-pore structure.[14,15]

The incomplete conversion from the HT to LT phase is under investigation, but it is likely due to either defects or residual strain present in the crystallites hindering the complete conversion to the monoclinic phase.

Upon warming the sample from 77 to 295 K and once again measuring the diffraction pattern, there is very little to distinguish these two data sets. Rietveld refinement analysis (Figure 1(b)) shows that not only is the LT phase retained on heating, but the phase fraction is nominally the same as that at 77 K. Although the diffraction patterns of MIL-53(Al) in Figure 1 are both collected at 295 K, the striking differences between the patterns indicates that the structures at room temperature are quite different and depend on the thermal history. This temperature dependent phase transition and hysteresis of MIL-53(Al) has not been reported before, and to the best of our knowledge, this is the first observation of temperature inducing such a large hysteretic phase transition in a metal-organic framework.

The diffraction patterns shown in Figure 1 demonstrate the large changes in pore size associated with the structural transition. The intense and well-isolated (011) Bragg peak at ~12° in the HT phase corresponds to diffraction from the Bragg planes defined by the rhombic pore walls of MIL-53 HT. The intensity of this reflection is directly proportional to the fraction of the open-pored HT phase in the sample. Comparing the relative intensities of the (011) HT reflections between Figure 1, parts b and a, it is evident that the Figure 1b pattern contains a much smaller amount of the HT structure, even though both patterns were collected at room temperature. The corresponding Bragg plane of the LT phase is the (110) reflection at around 18° in Figure 1b only, the second most intense reflection for this phase. Such a large shift in peak position arising from structurally similar Bragg planes clearly indicates the dramatic pore size change: the longer axis is slightly elongated from ~17 Å to ~21 Å, while the shorter axis is shrunk by almost a factor of 2, from ~13 Å to ~7 Å. Conversely, the periodicity of the 1-D channels is robust, varying only slightly through this transition, corresponding to the unit-cell length of the *a*-axis and *c*-axis for the HT and LT phases, respectively.

In order to identify the driving force for the HT-LT phase transition, we probed the low energy phonons using inelastic neutron scattering. We first compared the room temperature INS spectra of MIL-53(Al) in the two different phases using the DCS spectrometer (Figure 2, left panel). The diffraction patterns (Figure 2, right panel) are simultaneously obtained over the limited Q range when measuring the INS spectra. The diffraction patterns are in agreement with the proposed structural models and clearly indicate that the HT phase has changed to the LT phase upon quenching and returning to room temperature. The INS spectrum of the HT phase shows a strong low-energy excitation close to −5 meV energy transfer. Upon transition to the LT phase, the density of states of this feature decreases significantly and hence can be associated with the structural change. While the physical origin of this excitation will be addressed later in this paper, we can use the intensity of the excitation at −5 meV as a useful indicator of the phase composition of MIL-53(Al). We used the FCS spectrometer to collect INS data at several temperatures while cooling from 450 K down to 77 K and then upon heating to 390 K. To ensure the sample was at equilibrium during these experiments, we waited more than

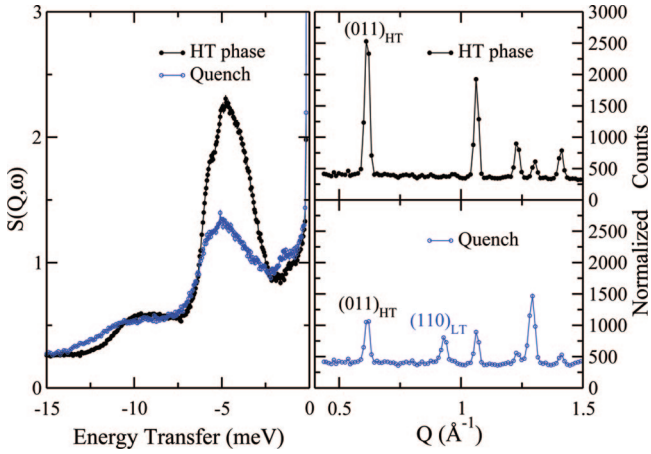

Figure 2. (Left panel) Inelastic neutron scattering spectra of MIL-53(Al) measured at room temperature for the HT phase (solid circles) and the predominantly LT phase (open circles, labeled "Quench"). (Right panel) Simultaneously measured diffraction patterns of the HT and LT phases with the largest *d*-spacing reflections noted for each phase. Error bars indicate one standard deviation of the counting statistics.

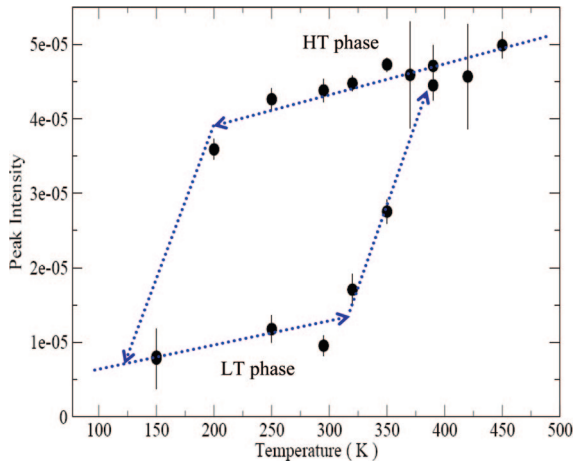

Figure 3. Structural hysteresis diagram of MIL-53(Al) identified using inelastic neutron scattering data measured on the FCS spectrometer. The transition temperature from the HT phase to the LT phase occurs around 125 K, while the transition from the LT phase to the HT phase happens gradually between 325 to 375 K. Error bars indicate one standard deviation from integrating over the −5 meV INS feature. The possible transition temperature from the HT phase to LT phase is further restricted than evidenced by the data, to between 125 to 150 K, using data from the FANS instrument. (See text for details.) The dashed lines are drawn as a guide to the eye.

30 min at each temperature and each measurement took over 10 h. Figure 3 shows the extracted peak area of the −5 meV feature as a function of the cycled temperature.

At 450 K, we have established that MIL-53(Al) is in the HT phase and the corresponding intensity of the low-energy peak in the INS spectrum is relatively large. With decreasing temperature, the peak intensity decreases slightly indicating that the HT phase remains the majority phase. After the sample was measured at 200 K, the sample was cooled to 77 K (for about 2 h) and then warmed to 150 K. The INS peak intensity becomes significantly smaller indicating that the majority of the sample has transformed to the LT phase. Using this data, we can only identify the phase transition happening between 77 and 200 K. However, we have further narrowed the transition temperature to between 125 and 150 K for our particular MIL-53(Al) sample. (see Supporting Information for details, Figure S3) Upon further increase in temperature, the peak intensity remains relatively small indicating the predominant presence of LT phase with a transition to HT phase occurring between 325 and 375 K.

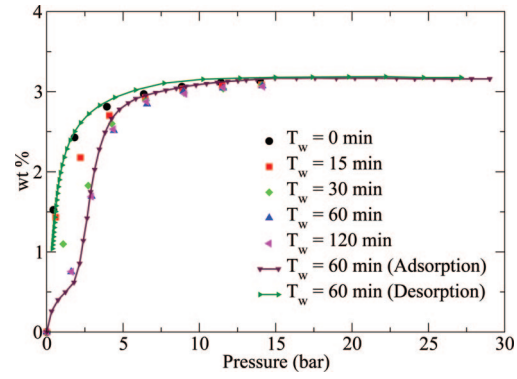

Figure 4. Hydrogen excess adsorption isotherms of MIL-53(Al) measured at 77 K. The empty volume is calibrated at room temperature for a sample at the HT phase. The coarsely spaced data are for different waiting times, T_w, at 77 K before measuring the isotherms. The full isotherms were measured after waiting 60 min at 77 K, illustrating how the slow dynamics of the structural transitions of MIL-53(Al) affects the adsorption measurements.

We also note that the transition rate is slow. For example, after preparing the sample at the HT phase first and quenching the sample cell in liquid N_2 for 20 min during the INS experiments, there is little change in the INS spectrum from that representative of the HT phase (see Supporting Information, Figure S4).

The combined effects of the structural transitions, together with the slow transition rate, must significantly affect volumetric gas adsorption measurements, especially those for hydrogen storage measurements: (1) the volumetric method commonly used for high pressure hydrogen adsorption measurement requires the accurate determination of the internal volume of a sample to calculate the excess adsorption. A pore size that varies with both temperature and gas pressure in such a fashion as determined here implies that the empty volume also changes while measuring the isotherm. Thus, using a fixed empty volume determined with He gas at room temperature cannot result in an accurate adsorption capacity; (2) the slow dynamics for the structural transition is comparable to the time scale of a typical isotherm measurement that will also impart a time-of-measurement dependence to the isotherm.[20] We illustrate this effect in Figure 4, where we sequentially quench a HT phase sample to 77 K and wait a period, T_w, before starting a hydrogen adsorption isotherm measurement. The T_w dependent isotherms are very different due to the slow dynamics of the structural phase transition of MIL-53(Al). When $T_w = 0$ min, the coarsely sampled isotherm is typical of an isotherm in a material with rigid open pores. With increasing T_w, there is a reduction in the low-pressure adsorption capacity that becomes essentially the same between $T_w = 60$ min and $T_w = 120$ min. Therefore, it seems that it takes about one hour to convert the sample to the predominantly-LT phase. The H_2 adsorption/desorption isotherm was measured again with finer steps at $T_w = 60$ min. We can surmise that the low-pressure hump in the isotherm

(20) It should be noted that the observed structural transition time is also affected by the thermal conductivity of the sample. With changes in the amount of sample or particle size, the measured transition time may change, but is still expected to be slow (on the order of an hour).

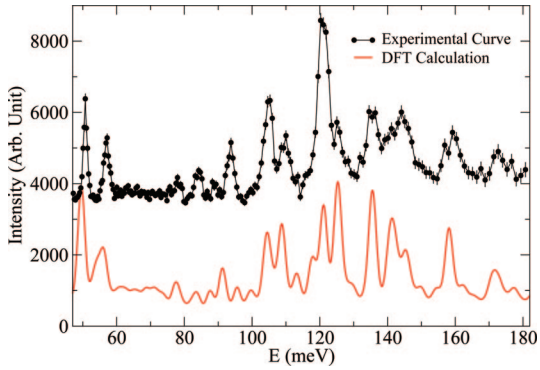

Figure 5. Comparison of the high energy inelastic neutron scattering data for MIL-53(Al) in the LT phase (circles) and that predicted from the DFT calculation (solid line). Data are displaced for clarity. Error bars for the experimental data indicate one standard deviation of the counting statistics.

is the closed-pored LT phase undergoing expansion to a more open pore, potentially similar to the HT-phase. In particular, the final desorption curve is almost identical with the adsorption curve at $T_w = 0$ min, indicating that during desorption, the structure of MIL-53 seems to remain open. The possibility of having an adsorbate that does not cause MIL-53(Al) to adopt the closed-pored LT phase is quite different from what has been presented in the literature and will be probed further using neutron diffraction where adsorption sites of D_2 can be identified.[3,4,21−23] Additionally, if the maximum of the isotherm corresponds to an open-pored HT structure, then careful manipulation of the sample prior to measuring the void volume can potentially result in the correct excess adsorption capacity of material, if not, the shape of the isotherm and the correct isosteric heat of adsorption.

To understand the physical origin of the structural transition, we employed first-principle calculations that have proven useful in understanding the physical properties of MOFs and optimizing framework interactions with adsorbates.[24] The total energy of the LT and HT structures was minimized at the experimental lattice parameters and we proceeded to calculate the dynamical properties of the two structures. Figure 5 shows the comparison of the calculated density of states of MIL-53 framework in the LT phase together with the experimental results obtained from inelastic neutron scattering (see Supporting Information). The general agreement indicates the fair accuracy of our calculation in the current energy range. Experimentally, the intensity of the vibrational peaks at ∼50.8 meV and ∼57.1 meV is observed to be dependent upon the structural transition, (see Supporting Information, Figure S5), and corresponds to twisting modes of the benzene ring. Hence, it is reasonable to speculate that the structural transition is strongly coupled to, and possibly triggered by, the low energy librational motions of the benzene ring.

Inspection of the dynamical calculation of the HT phase indicates a large amplitude twisting motion of the benzene rings at energy transfers of 3.5 and 6.1 meV. These motions would correspond to the signature INS peak shown in Figure 2 and previously used as a measure of the total HT phase in determining the hysteresis curve. In the LT phase structure, a similar motion of the organic chain is calculated at a somewhat higher frequency of 10.3 meV. While it is difficult to be overly confident in assigning a zero Kelvin calculation to a phase transition that occurs at high temperature, we interpret this as an indication of the involvement of these modes in the total energy consideration. Physically, the higher energy benzene-twist mode in the LT phase can be seen as becoming rather restricted in amplitude with increasing temperature due to the proximity of neighboring benzene rings. The repulsion of the neighboring rings is eventually relaxed upon the transition to the HT phase where the benzene librations are somewhat softened and increase in intensity/amplitude. Again, while this is certainly a contribution to the Gibbs free energy of the system, other contributions such as phonon populations may play significant roles. In fact, we have also identified another potential contribution arising from difference in the distortion from the octahedral AlO_6 clusters in the LT and HT phases. Such observations are quite common in crystallography and a convenient parametrization has been previously developed[25] and applied here (see Supporting Information, Figure S6). We also note the family of MIL-53 materials with alternate metal oxide clusters and/or napthalenedicarboxylate ligands show either dissimilar high temperature desolvation characteristics or N_2 adsorption behaviors at 77 K. This may imply that both the metal and nature of the ligand can have an affect on the phase transition.[26−28]

In the current paper, we have reported that MIL-53(Al) can be converted to a closed-pored LT phase by only decreasing temperature and without the aid of any guest molecules. This provides a different way to control the porosity in MIL-53 other than by adsorbing guest molecules and may be applicable to other metal-organic framework-type breathing structures. A very large hysteresis as a function of temperature is observed. The transition from the HT phase to the LT phase is observed between 125 and 150 K, while the transition from the LT phase to HT phase occurs between 325 and 375 K. This large hysteresis may be useful for designing temperature controlled smart materials. An important impact of this is that we cannot know, a priori, the structural composition of a bare material without the knowledge of its thermal history. This becomes especially important for gas adsorption isotherm experiments using the volumetric method, where one usually has to measure the empty volume of a sample, which is typically obtained at room temperature with low-pressure helium gas. In order to correctly relate the empty volume information to the correct structure of MIL-53(Al), we have to clearly understand its thermal history and relate that to the phase diagram that has the potential to be different for each synthesized material and also dependent on heating/cooling rates. The observed slow transition rate also significantly affects the hydrogen adsorption/desorption isotherm.

(21) Liu, Y.; Kabbour, H.; Brown, C. M.; Neumann, D. A.; Ahn, C. C. *Langmuir* **2008**, *24*, 4772.
(22) Peterson, V. K.; Liu, Y.; Brown, C. M.; Kepert, C. J. *J. Am. Chem. Soc.* **2006**, *128*, 15578.
(23) Yildirim, T.; Hartman, M. R. *Phys. Rev. Lett.* **2005**, *95*, 215504.
(24) Zhou, W.; Yildirim, T. *Phys. Rev. B* **2006**, *74*, 180301.
(25) Robinson, K.; Gibbs, G. V.; Ribbe, P. H. *Science* **1971**, *172*, 567.
(26) Millange, F.; Serre, C.; Cuillou, N.; Férey, G.; Walton, R. I. *Angew. Chem., Int. Ed.* **2008**, *47*, 4100–4105.
(27) Horcajada, P.; Serre, C.; Maurin, G.; Ramsahye, N. A.; Balas, F.; Vallet-Regí, M.; Sebban, M.; Taulelle, F.; Férey, G. *J. Am. Chem. Soc.* **2008**, *130*, 6774–6780.

Acknowledgment. The authors thank J. Leão and S. Slifer for experimental assistance, M. A. Green for useful discussion, and Dr. Keith Refson at the Rutherford Appleton Laboratory. This work was partially supported by the U.S. Department of Energy's Office of Energy Efficiency and Renewable Energy within the Hydrogen Sorption Center of Excellence.

Supporting Information Available: Additional information including Rietveld analysis details, neutron vibrational spectroscopy experiments, tables for the Rietveld analysis results at different temperatures, Figures for the diffraction patterns at 450 and 77 K, and INS spectra at different temperatures. This material is available free of charge via the Internet at http://pubs.acs.org.

JA803669W

(28) Loiseau, T.; Mellot-Draznieks, C.; Muguerra, H.; Férey, G.; Haouas, M.; Taulelle, F. *C. R. Chimie* **2005**, *8*, 765–772.